

Impact ionization scattering model based on the random-k approximation for GaAs, InP, InAlAs, and InGaAs

Denis Dolgos, Andreas Schenk, and Bernd Witzigmann

Citation: *J. Appl. Phys.* **111**, 073714 (2012); doi: 10.1063/1.3699313

View online: <http://dx.doi.org/10.1063/1.3699313>

View Table of Contents: <http://jap.aip.org/resource/1/JAPIAU/v111/i7>

Published by the [American Institute of Physics](#).

Related Articles

Effect of bending stress on structures and quantum conduction of Cu nanowires

Appl. Phys. Lett. **100**, 123107 (2012)

Theory of charging and charge transport in “intermediate” thickness dielectrics and its implications for characterization and reliability

J. Appl. Phys. **111**, 054112 (2012)

Evolution of deep electronic states in ZnO during heat treatment in oxygen- and zinc-rich ambients

Appl. Phys. Lett. **100**, 112108 (2012)

Iron-phthalocyanine molecular junction with high spin filter efficiency and negative differential resistance

J. Chem. Phys. **136**, 064707 (2012)

Length dependence of the resistance in graphite: Influence of ballistic transport

J. Appl. Phys. **111**, 033709 (2012)

Additional information on J. Appl. Phys.

Journal Homepage: <http://jap.aip.org/>

Journal Information: http://jap.aip.org/about/about_the_journal

Top downloads: http://jap.aip.org/features/most_downloaded

Information for Authors: <http://jap.aip.org/authors>

ADVERTISEMENT



**FIND THE NEEDLE IN THE
HIRING HAYSTACK**

Post jobs and reach
thousands of hard-to-find
scientists with specific skills



<http://careers.physicstoday.org/post.cfm> **physicstoday** JOBS

Impact ionization scattering model based on the random- \mathbf{k} approximation for GaAs, InP, InAlAs, and InGaAs

Denis Dolgos,^{1,a)} Andreas Schenk,¹ and Bernd Witzigmann²

¹*Integrated Systems Laboratory, ETH Zurich, Gloriastrasse 35, Zurich 8092, Switzerland*

²*Computational Electronics and Photonics Group, University of Kassel, Wilhelmshöher Allee 71, Kassel 34121, Germany*

(Received 24 January 2012; accepted 28 February 2012; published online 10 April 2012)

The inclusion of momentum conservation and the evaluation of the double Coulomb transition matrix elements render the calculation of the impact ionization scattering rates with first principle approaches computationally expensive and their numerical implementation laborious. Despite the positive assessment of Kane's random- \mathbf{k} approximation, the impact ionization rates and the secondary carrier energies for the III-V semiconductors GaAs, InP, In_{0.52}Al_{0.48}As, and In_{0.53}Ga_{0.47}As have not been provided to the charge transport modeling community in terms of analytical fit functions yet. We provide the impact ionization scattering rates as modified Keldysh formulas and the secondary carrier energies as straight line fits. The band structure computation is based on the empirical pseudopotential method. © 2012 American Institute of Physics. [<http://dx.doi.org/10.1063/1.3699313>]

I. INTRODUCTION

Models for the calculation of the impact ionization scattering rates, starting from Fermi's golden rule, vary widely in literature. For example, Kane,¹ Jung *et al.*,² and Kuligk *et al.*³ computed the impact ionization rate evaluating the detailed matrix elements, the dielectric function, and took momentum conservation into account. Kane introduced the random- \mathbf{k} approximation¹ (RKA), which neglects momentum conservation. Sano and Yoshii⁴ additionally introduced an approximation that assumes mean secondary carrier energies. Some full-band Monte Carlo (FBMC) works utilize a modified Keldysh formula, which is a fit to the impact ionization rate of first principle approaches. At the advent of FBMC simulations, and interestingly even later, the Keldysh approximation, valid for parabolic band structures, was used for the calculation of the impact ionization rates despite the existence of Kane's computationally simple RKA.⁵⁻⁷

The magnitude of the impact ionization scattering rate depends on the volume of the available phase space and the average squared transition matrix element $|M_{ii}|^2$ within that phase space. In indirect gap materials, the mean matrix elements are insensitive to the impacting carrier energy. In direct gap materials, the constant matrix approximation (CMA) underestimates the rate at low impacting carrier energies (by up to two orders of magnitude for InGaAs [Ref. 8]). Kane's RKA works better for indirect gap semiconductors than for direct gap semiconductors.⁹ Momentum conservation allows for a large number of possible final \mathbf{k} -states due to the 48-fold symmetry of the cubic lattice. Practically, the large set of final \mathbf{k} -states will scatter randomly throughout the Brillouin zone. Additionally, the three multi-dimensional integrals (sums) over the \mathbf{k} -space (see Eq. (1)) considerably average the details of the band structure.¹ The RKA and CMA take

advantage of these two properties and highly reduce the complexity of the impact ionization rate computation from a computational and implementational point of view. The RKA and CMA reduce the nine-dimensional integration over the δ -function in the reciprocal space to a two-dimensional integral over one-particle density of states (DOS) in the energy space. In this paper, the costly computation of the Coulomb transition matrix elements is bypassed by tuning it to experimental data,¹⁰ with our FBMC simulator *CarloS* described in Ref. 11. The application of the RKA and CMA is an appealing possibility to compute the impact ionization rate with a manageable effort and to keep agreement with first principle methods.^{1,10,12} Compared to the approach of Sano *et al.*,⁴ Kane's RKA provides information about the secondary carrier energies and makes additional fit parameters needless. The additional implementation work for the RKA- and CMA-based rate calculation compared to the implementation work of the approach of Sano *et al.* (Ref. 4) is marginal. The use of the modified Keldysh formula provided by first principle methods is a viable option for Monte Carlo (MC) charge transport simulations of the well-known material GaAs. In addition, for GaAs, the secondary carrier energies are provided in the literature (e.g., Ref. 2). For the materials InP, In_{0.52}Al_{0.48}As (InAlAs), and In_{0.53}Ga_{0.47}As (InGaAs), the impact ionization scattering rates and the secondary carrier energy distributions are not available in the literature. First principle evaluations concentrate on materials like Si, GaAs, or GaN. Furthermore, the selection of the final \mathbf{k} -states in the RKA and CMA is computationally efficient for FBMC simulations.¹³

The importance of the impact ionization rate around the threshold energy depends on the high energy tail of the carrier distribution and the ratio of the impact ionization rate to the phonon scattering rates. A carrier, being able to impact-ionize, has to survive to energies above the threshold, emitting less phonons than the bulk of the particles. The carrier

^{a)}Electronic mail: dolgos@iis.ee.ethz.ch.

distribution above the threshold energy therefore strongly depends on the dissipation processes below the threshold energy. If the carrier has survived to impact ionization enabling energies, the occurrence of impact ionization has to be relevant compared to phonon scattering. However, compared with phonon scattering, impact ionization is of no practical importance at energies around the threshold.^{1,8} The RKA is considered to be “excellent”^{9,10} because it provides agreement over many orders of magnitude as if no approximation is involved for energies where impact ionization is a relevant scattering mechanism. Interestingly, despite the positive assessment of the RKA and over 360 citations of Kane’s work,¹ to the best of the authors’ knowledge, the impact ionization rates and the secondary carrier energies have not been provided to the MC transport modeling community in terms of analytical fit functions yet.

II. IMPACT IONIZATION SCATTERING MODEL

Impact ionization is an electron-electron interaction process. A high-energy carrier is able to generate a new electron-hole pair by lifting an electron from the valence band into the conduction band. The transition probability follows from Fermi’s golden rule. For a primary impacting electron, the impact ionization scattering rate is given by¹

$$W_{ii}(\mathbf{k}_c) = \frac{2\pi}{\hbar} \sum_{\substack{v', c', c'' \\ c'' \geq c'}} \sum_{\mathbf{k}_c', \mathbf{k}_c'', \mathbf{k}_c'''} |M_{ii}|^2 \delta(E_c(\mathbf{k}_c) - E_{c'}(\mathbf{k}_c') - E_{c''}(\mathbf{k}_c'') - E_g) \delta_{\mathbf{k}_c, \mathbf{k}_c' + \mathbf{k}_c'' + \mathbf{k}_c''' + \mathbf{G}}, \quad (1)$$

with the reduced Planck constant \hbar , the double Coulomb impact ionization matrix element M_{ii} , and the sum over all possible final \mathbf{k} -states and the conduction c and the valence bands v . The prime indicates the states after scattering. Furthermore, E_c and E_v denote the full-band energy of electrons and holes, respectively, and E_g is the bandgap energy. Swapping c and v in Eq. (1) leads to the scattering rate for a primary impacting hole. In first principle approaches, $|M_{ii}|^2 = |M_d|^2 + |M_e|^2 + |M_d - M_e|^2$ is calculated with the direct term M_d , the exchange term M_e , and the Coulomb interaction potential $V(\mathbf{r}_1, \mathbf{r}_2)$ according to²

$$M_d = \iint d^3\mathbf{r}_1 d^3\mathbf{r}_2 \Psi_1^*(\mathbf{r}_1) \Psi_2^*(\mathbf{r}_2) V(\mathbf{r}_1, \mathbf{r}_2) \Psi_1(\mathbf{r}_1) \Psi_2(\mathbf{r}_2), \quad (2a)$$

$$M_e = \iint d^3\mathbf{r}_1 d^3\mathbf{r}_2 \Psi_2^*(\mathbf{r}_1) \Psi_1^*(\mathbf{r}_2) V(\mathbf{r}_1, \mathbf{r}_2) \Psi_1(\mathbf{r}_1) \Psi_2(\mathbf{r}_2), \quad (2b)$$

with the carrier position \mathbf{r} . Here, $\Psi_{1,2}$ and $\Psi_{1',2'}$ denote the wave functions of the initial and the final state, respectively.

We utilize the empirical pseudopotential method (EPM)^{14,15} to compute the full-band structure with parameters taken from Chelikowsky and Cohen¹⁴ and Zheng *et al.*¹⁶ Because of the empirical properties of the EPM, the agree-

ment with experimental data is better than using methods with *ab initio* potentials. *Ab initio* calculations of the band structure utilize other severe approximations, e.g., for the exchange and the correlation interactions, which render the agreement with experiment worse. In this work, we calculate the impact ionization scattering rates using the RKA,¹ which ignores momentum conservation. Dropping the restriction of momentum conservation leads to an upper bound estimation of the impact ionization scattering rate. The inclusion of the unities $1 = \int_0^\infty dE_{c'} \delta(E_{c'} - E_{c'}(\mathbf{k}_{c'}))$ and $1 = \int_0^\infty dE_{v'} \delta(E_{v'} - E_{v'}(\mathbf{k}_{v'}))$ ¹⁷ into Eq. (1) and the following summation over $\mathbf{k}_{c'}$ and $\mathbf{k}_{v'}$ yields the impact ionization scattering rate in the RKA and CMA. Comparing Kane’s RKA with first principle impact ionization evaluation methods, the RKA- and CMA-based impact ionization rates provide good results.^{1,10,12}

For a primary impacting electron and hole, the rate is given by^{1,18}

$$W_{ii}(E_c(\mathbf{k}_c)) = \Lambda_e^{ii} \mathcal{D}_{ii}(E_c), \quad (3a)$$

$$W_{ii}(E_v(\mathbf{k}_v)) = \Lambda_h^{ii} \mathcal{D}_{ii}(E_v). \quad (3b)$$

Here, the \mathcal{D}_{ii} are the density of states overlap integrals defined in Eqs. (5a) and (5b). The prefactors Λ^{ii} include the averaged matrix element M_{ii} ,

$$\Lambda^{ii} = \frac{2\pi}{\hbar} |M_{ii}|^2 \frac{V^3}{N_{\text{cell}}}, \quad (4)$$

with the crystal volume V and the number of unit cells N_{cell} . In the RKA and CMA, the impact ionization prefactors Λ_e^{ii} and Λ_h^{ii} are treated as fit parameters, which are tuned to experimental data of the impact ionization coefficients of electrons and holes. We use our FBMC simulator *CarloS* for this calibration. Bulman *et al.*^{19,20} and Millidge *et al.*²¹ provide the experimental data for GaAs. Cook *et al.*²² and Taguchi *et al.*²³ offer the experiments for InP. We have taken the data for InAlAs from Watanabe *et al.*²⁴ and for InGaAs from Osaka *et al.*²⁵ Concerning the details of the calibration process, we refer to Dolgos *et al.*¹¹

A. Computation of scattering rates

The impact ionization scattering rate has a functional dependency on a quantity we call density of states overlap integral \mathcal{D}_{ii} . For an impacting electron and hole, this function is given by¹

$$\mathcal{D}_{ii}(E_c) = \sum_{\substack{v', c', c'' \\ c'' \geq c'}} \int_0^{\hat{E}_{c'}} dE_{c'} \int_0^{\hat{E}_{v'}} dE_{v'} \mathcal{D}_{v'}(E_{v'}) \mathcal{D}_{c'}(E_{c'}) \times \mathcal{D}_{c''}(E_c - E_{c'} - E_{v'} - E_g), \quad (5a)$$

$$\mathcal{D}_{ii}(E_v) = \sum_{\substack{c', v', v'' \\ v'' \geq v'}} \int_0^{\hat{E}_{v'}} dE_{v'} \int_0^{\hat{E}_{c'}} dE_{c'} \mathcal{D}_{c'}(E_{c'}) \mathcal{D}_{v'}(E_{v'}) \times \mathcal{D}_{v''}(E_v - E_{v'} - E_{c'} - E_g). \quad (5b)$$

The two secondary electrons or holes are indistinguishable; the indices of summation have the constraint $c'' \geq c'$ or

$v'' \geq v'$, respectively. The upper integration boundaries are for an impacting electron

$$\hat{E}_{c'} = E_c(\mathbf{k}_c) - E_g, \quad (6a)$$

$$\hat{E}_{v'} = E_c(\mathbf{k}_c) - E_{c'} - E_g, \quad (6b)$$

and for an impacting hole

$$\hat{E}_{v'} = E_v(\mathbf{k}_v) - E_g, \quad (7a)$$

$$\hat{E}_{c'} = E_v(\mathbf{k}_v) - E_{v'} - E_g. \quad (7b)$$

For the numerical computation, the discretized versions of Eqs. (5a) and (5b),

$$\begin{aligned} \mathcal{D}_{ii}(E_c) = & \sum_{\substack{c' \geq c \\ v' \geq v''}} \sum_{i=0}^{i_{\max}^c} \sum_{j=0}^{j_{\max}^c} \mathcal{D}_{v'}(E_j) \Delta E_j \mathcal{D}_{c'}(E_i) \Delta E_i \\ & \times \mathcal{D}_{c''}(E_c - E_i - E_j - E_g), \end{aligned} \quad (8a)$$

$$\begin{aligned} \mathcal{D}_{ii}(E_v) = & \sum_{\substack{c' \geq v'' \\ v' \geq v''}} \sum_{i=0}^{i_{\max}^v} \sum_{j=0}^{j_{\max}^v} \mathcal{D}_{c'}(E_j) \Delta E_j \mathcal{D}_{v'}(E_i) \Delta E_i \\ & \times \mathcal{D}_{v''}(E_v - E_i - E_j - E_g), \end{aligned} \quad (8b)$$

are utilized with $i_{\max}^c = \text{int}(\hat{E}_{c'}/\Delta E_i)$, $j_{\max}^c = \text{int}(\hat{E}_{v'}/\Delta E_j)$, $i_{\max}^v = \text{int}(\hat{E}_{v'}/\Delta E_i)$, and $j_{\max}^v = \text{int}(\hat{E}_{c'}/\Delta E_j)$. The impact ionization scattering rate is dominated by the single particle DOS. Concerning the details of the DOS evaluation with the Gilat-Raubenheimer method, we refer to Refs. 11 and 26.

First principle evaluations of the impact ionization rates are provided to the community as piecewise-defined, modified Keldysh formulas,²

$$W_{ii}(E) = \Lambda^{ii}(E - E_{\text{th}})^\gamma, \quad (9)$$

with the threshold energy E_{th} . In this work, the modified Keldysh formula is defined on three energy intervals I, II, and III according to

$$\text{energy interval} = \begin{cases} \text{I} & \text{if } E_{\text{th}} \leq E \leq E_1, \\ \text{II} & \text{if } E_1 \leq E \leq E_2, \\ \text{III} & \text{if } E_2 \leq E. \end{cases} \quad (10)$$

The parameters Λ^{ii} , γ , E_1 , and E_2 are adjusted to possess a best straight line fit through

$$\tilde{W} = \gamma \tilde{E} + \tilde{\Lambda}, \quad (11)$$

with

$$\tilde{W} = \ln(W_{ii}), \quad (12a)$$

$$\tilde{E} = \ln(E - E_{\text{th}}), \quad (12b)$$

$$\tilde{\Lambda} = \ln(\Lambda^{ii}), \quad (12c)$$

and small modifications to assure a continuous rate function at the boundaries E_1 and E_2 . The parameters γ and E_{th} are fitted against the numerically evaluated DOS overlap integral \mathcal{D}_{ii} . The inclusion of the momentum conservation leads to a threshold energy being higher than the bandgap energy. In

TABLE I. Energy boundaries for the fits of the modified Keldysh formula. The threshold energies correspond to the particular band gap energies.

Material	E_{th} (eV)	E_1 (eV)	E_2 (eV)
GaAs	1.42	1.82	4.5
InP	1.34	2.08	4.84
InAlAs	1.46	2.40	5.53
InGaAs	0.74	2.02	6.0

the RKA, simply $E_{\text{th}} = E_g$ holds true. We fit the parameters Λ^{ii} such that the FBMC-evaluated impact ionization coefficients agree with the experimental data. Table I shows the threshold energies and the defined boundaries E_1 and E_2 of the energy intervals. A comparison of the full-band DOS of the different FBMC simulators in the literature shows that the utilized band structures vary especially for the DOS with contributions from higher conduction bands ($c \geq 2$). The nine-dimensional integration over the \mathbf{k} -space considerably averages the details of the underlying band structure. Therefore, the functional characteristic of the impact ionization rate, being fit to $(E - E_{\text{th}})^\gamma$, does not depend strongly on the details of the dispersion relation. Figure 1 illustrates a comparison of the impact ionization scattering rates calculated with different methods for impacting electrons in GaAs. The scattering rates computed with RKA-based methods are taken from Saravia and Duomarco²⁷ and Cavassilas *et al.*²⁸ The scattering rates using first principle calculations are given in Jung *et al.*² and Harrison *et al.*²⁹ In good approximation, it is possible to adjust the rate strength to make the scattering rates congruent for energies (>3 eV), where impact ionization is a relevant scattering mechanism. The strength of the rate Λ^{ii} is very sensitive to the individual Monte Carlo calibration, in particular, to the carrier-phonon coupling strength.¹⁰ Therefore, the exponent γ , defining the functional characteristic of the rate, has to be understood as being mainly determined by the band structure. In contrast to γ , the rate strength Λ^{ii} is viewed as a strongly calibration-dependent fit parameter based on the particular calibration of the phonon deformation potentials used in this work. Therefore, Λ^{ii} may be rather used as a fitting parameter in the MC

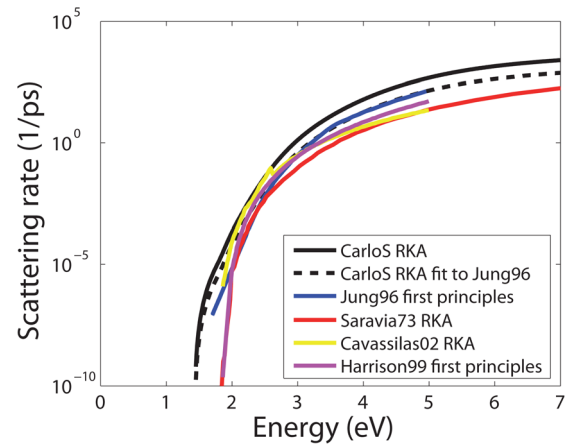


FIG. 1. Comparison of the impact ionization rates for primary impacting electrons in GaAs calculated with RKA-based methods (*CarloS*, Saravia 1973 (Ref. 27), Cavassilas 2002 (Ref. 28), and first principle approaches (Jung 1996 (Ref. 2), Harrison 1999 (Ref. 29)).

TABLE II. Fit parameters of the modified Keldysh formulas to the RKA-based calculation of the impact ionization scattering rates in the three energy intervals I, II, and III. The subscripts e and h indicate the parameters for electrons and holes, respectively.

Material	Fit parameter	I	II	III
GaAs	$\Lambda_e^{\text{ii}}(\text{ps}^{-1}\text{eV}^{-\gamma_e})$	5.53×10^{-4}	2.62×10^{-2}	2.31
	$\gamma_e(1)$	3.94	8.15	4.17
	$\Lambda_h^{\text{ii}}(\text{ps}^{-1}\text{eV}^{-\gamma_h})$	4.02×10^{-1}	4.72	6.68×10^1
	$\gamma_h(1)$	3.93	6.61	4.26
InP	$\Lambda_e^{\text{ii}}(\text{ps}^{-1}\text{eV}^{-\gamma_e})$	1.26×10^{-3}	4.67×10^{-3}	8.86×10^{-1}
	$\gamma_e(1)$	3.90	8.24	4.05
	$\Lambda_h^{\text{ii}}(\text{ps}^{-1}\text{eV}^{-\gamma_h})$	2.33	5.20	3.50×10^2
	$\gamma_h(1)$	4.01	6.68	3.32
InAlAs	$\Lambda_e^{\text{ii}}(\text{ps}^{-1}\text{eV}^{-\gamma_e})$	3.55×10^{-4}	4.87×10^{-4}	1.10×10^{-1}
	$\gamma_e(1)$	3.79	9.16	5.30
	$\Lambda_h^{\text{ii}}(\text{ps}^{-1}\text{eV}^{-\gamma_h})$	9.58×10^{-1}	1.13	7.86×10^1
	$\gamma_h(1)$	4.19	6.99	3.96
InGaAs	$\Lambda_e^{\text{ii}}(\text{ps}^{-1}\text{eV}^{-\gamma_e})$	5.41×10^{-5}	1.85×10^{-5}	4.51×10^{-3}
	$\gamma_e(1)$	5.19	9.53	6.22
	$\Lambda_h^{\text{ii}}(\text{ps}^{-1}\text{eV}^{-\gamma_h})$	7.46×10^{-3}	4.75×10^{-3}	1.19
	$\gamma_h(1)$	5.30	7.12	3.80

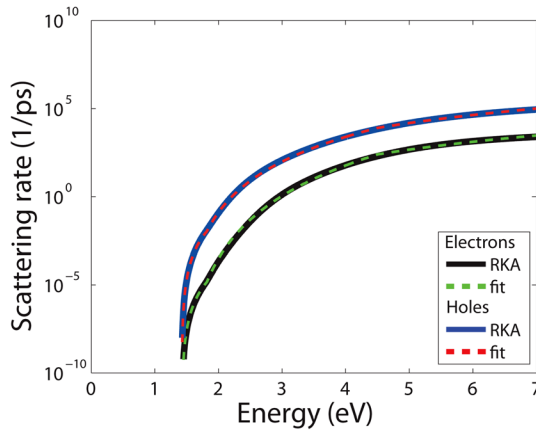
computations than γ . Table II summarizes the parameters of the impact ionization rate fits. Figure 2 presents the RKA-based impact ionization rates and the fitted, modified Keldysh formulas.

B. Computation of secondary carrier energies

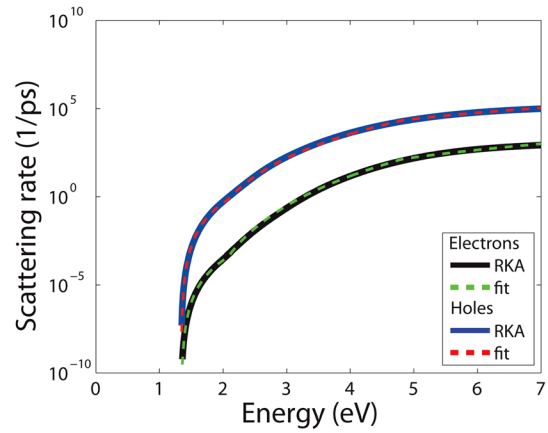
The secondary carrier energies after impact ionization are computed by means of the random- \mathbf{k} approximation too. The distribution functions for the secondary carrier energies W_{ee} and W_{hh} are given by¹

$$W_{ee}(E_c, E'_c) = \frac{2}{\mathcal{D}_{\text{ii}}(E_c)} \sum_{\substack{E'_c, E''_c \\ E'_c \geq E''_c}} \mathcal{D}_{c'}(E'_c) \times \int_0^{E_c - E'_c - E_g} dE_{v'} \mathcal{D}_{v'}(E_{v'}) \mathcal{D}_{c''}(E_c - E'_c - E_{v'} - E_g), \quad (13a)$$

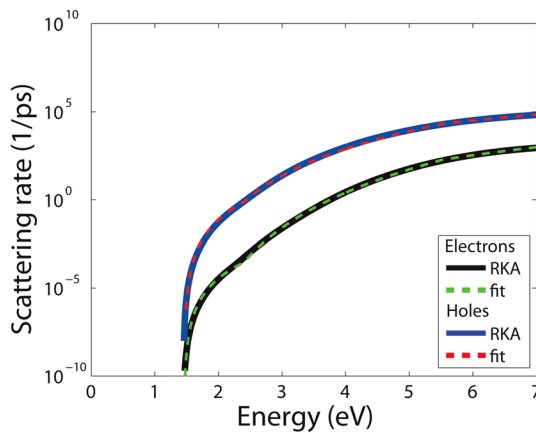
$$W_{hh}(E_v, E'_v) = \frac{2}{\mathcal{D}_{\text{ii}}(E_v)} \sum_{\substack{E'_v, E''_v \\ E'_v \geq E''_v}} \mathcal{D}_{v'}(E'_v) \times \int_0^{E_v - E'_v - E_g} dE_{c'} \mathcal{D}_{c'}(E_{c'}) \mathcal{D}_{v''}(E_v - E'_v - E_{c'} - E_g), \quad (13b)$$



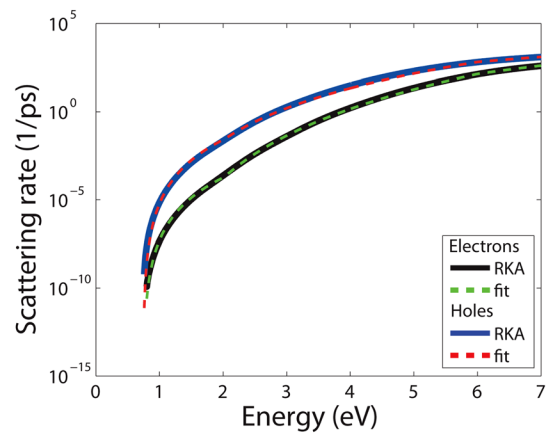
(a)



(b)



(c)



(d)

FIG. 2. Modified Keldysh formulas fitted to the calculated RKA-based impact ionization rates for electrons (e) and holes (h) of (a) GaAs, (b) InP, (c) InAlAs, and (d) InGaAs.

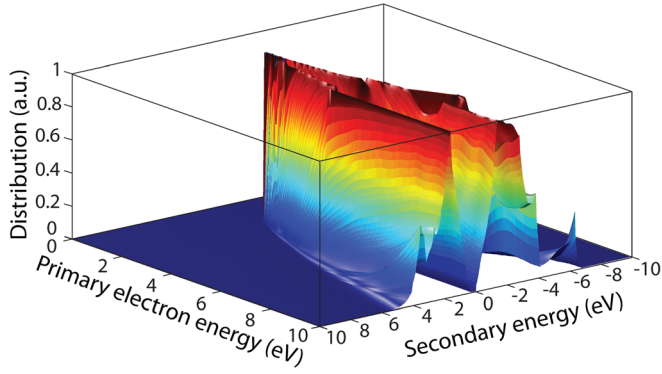


FIG. 3. Secondary carrier energy distribution function $W_{cc}(E_c, E'_c)$ computed using the random- \mathbf{k} approximation for an impacting electron in GaAs. The negative energies correspond to secondary holes.

with the primary electron/hole energy E_c/E_v and the secondary electron/hole energy E'_c/E'_v . Here, W_{ee} and W_{hh} are normalized to 2, because the secondary particles are indistinguishable.¹ Application of the rejection technique to Eqs. (13a) and (13b) generates the random variables E'_c and E'_v for the given primary energies E_c and E_v .³⁰ Figure 3 shows the secondary carrier energy distribution function $W_{cc}(E_c, E'_c)$ of GaAs. The mean values of the secondary energy distributions are given by

TABLE III. Parameters for the fits of the mean secondary carrier energies.

Material	m (1)	s (eV)
GaAs	0.350	-0.501
InP	0.292	-0.417
InAlAs	0.384	-0.518
InGaAs	0.264	-0.357

$$\langle E'_c \rangle(E_c) = \sum_{E'_c} W_{ee}(E_c, E'_c) E'_c, \quad (14a)$$

$$\langle E'_v \rangle(E_v) = \sum_{E'_v} W_{hh}(E_v, E'_v) E'_v. \quad (14b)$$

The mean energies of the secondary generated carriers are provided as straight line fits²:

$$\langle E'_c \rangle(E_c) = mE_c + s, \quad (15a)$$

$$\langle E'_v \rangle(E_v) = mE_v + s. \quad (15b)$$

Here, $\langle E'_{c,v} \rangle$ corresponds to the sum of the energies of the two indistinguishable secondary particles. Table III presents the fit parameters of the mean secondary carrier energies. Figure 4 shows the straight line fits with the RKA-based

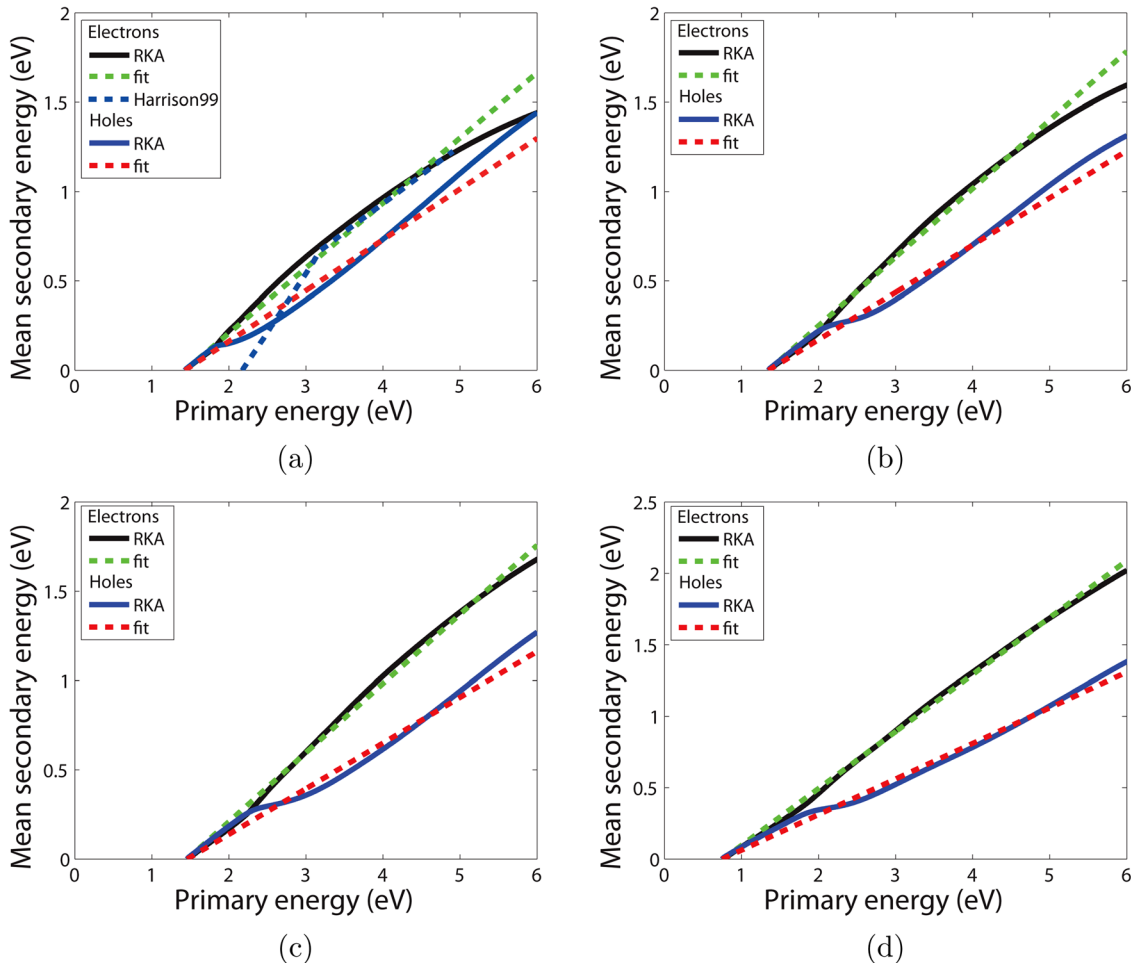


FIG. 4. Mean secondary energies fitted to the RKA-based mean secondary energy functions for (a) GaAs, (b) InP, (c) InAlAs, and (d) InGaAs. The mean energy of secondary electrons for an impacting electron in GaAs is compared with a first principle method published in Ref. 29.

calculations of the mean secondary carrier energies. For primary energies (>3 eV), where impact ionization is a relevant scattering mechanism compared to carrier-phonon scattering, the RKA-based computation agrees well with the first principle calculation of Harrison *et al.*²⁹ (see Fig. 4(a)).

For a primary impacting electron, the secondary carrier energies for the two electrons E'_{e1} , E'_{e2} , and the single hole E'_h can be approximated according to

$$E'_{e1} = \langle E'_c \rangle (E_c) r, \quad (16a)$$

$$E'_{e2} = \langle E'_c \rangle (E_c) - E'_{e1}, \quad (16b)$$

$$E'_h = E_c - \langle E'_c \rangle (E_c) - E_g, \quad (16c)$$

with a random number r between 0 and 1. For a primary impacting hole, the secondary carrier energies for the two holes E'_{h1} , E'_{h2} , and the single electron E'_e can be approximated corresponding to

$$E'_{h1} = \langle E'_v \rangle (E_v) r, \quad (17a)$$

$$E'_{h2} = \langle E'_v \rangle (E_v) - E'_{h1}, \quad (17b)$$

$$E'_e = E_v - \langle E'_v \rangle (E_v) - E_g. \quad (17c)$$

III. CONCLUSION

We have calculated the impact ionization scattering rates and the secondary carrier energies by means of the RKA and CMA for the III-V semiconductors GaAs, InP, InAlAs, and InGaAs. The application of the RKA and CMA is an appealing possibility to compute the impact ionization scattering rates with a manageable effort and to keep agreement with first principle methods. The costly computation of the Coulomb transition matrix elements is bypassed by tuning it to experimental data with our FBMC simulator. We provide the results as modified Keldysh formulas and straight line fits with tabulated parameters. For example, our results may be helpful for FBMC and multivalley MC approaches, which model materials with incomplete data of the impact ionization rates and secondary carrier energies.

¹E. O. Kane, "Electron scattering by pair production in silicon," *Phys. Rev.* **159**, 624–631 (1967).

²H. K. Jung, K. Taniguchi, and C. Hamaguchi, "Impact ionization model for full band Monte Carlo simulation in GaAs," *J. Appl. Phys.* **79**, 2473–2480 (1996).

³A. Kuligk, N. Fitzer, and R. Redmer, "Ab initio impact ionization rate in GaAs, GaN, and ZnS," *Phys. Rev. B* **71**, 085201 (2005).

⁴N. Sano and A. Yoshii, "Impact-ionization model consistent with the band structure of semiconductors," *J. Appl. Phys.* **77**, 2020–2025 (1995).

⁵M. V. Fischetti and S. E. Laux, "Monte Carlo analysis of electron transport in small semiconductor devices including band-structure and space-charge effects," *Phys. Rev. B* **38**, 9721–9745 (1988).

⁶K. F. Brennan, N. Mansour, and Y. Wang, "Simulation of advanced semiconductor devices using supercomputers," *Comput. Phys. Commun.* **67**, 73–92 (1991).

⁷G. M. Dunn, G. J. Rees, J. P. R. David, S. A. Plimmer, and D. C. Herbert, "Monte Carlo simulation of impact ionization and current multiplication in short GaAs diodes," *Semicond. Sci. Technol.* **12**, 111–120 (1997).

⁸D. Harrison, R. Abram, and S. Brand, "Characteristics of impact ionization rates in direct and indirect gap semiconductors," *J. Appl. Phys.* **85**, 8186–8192 (1999).

⁹J. Geist and W. Gladden, "Transition rate for impact ionization in the approximation of a parabolic band structure," *Phys. Rev. B* **27**, 4833–4840 (1983).

¹⁰M. V. Fischetti and S. E. Laux, "Monte Carlo simulation of electron transport in Si: The first 20 years," in *ESSDERC '96. Proceedings of the 26th European Solid State Device Research Conference* (IEEE, 1996), pp. 813–820.

¹¹D. Dolgos, H. Meier, A. Schenk, and B. Witzigmann, "Full-band Monte Carlo simulation of high-energy carrier transport in single photon avalanche diodes: Computation of breakdown probability, time to avalanche breakdown, and jitter," *J. Appl. Phys.* **110**, 084507 (2011).

¹²M. V. Fischetti, N. Sano, S. E. Laux, and K. Natori, "Full-band Monte Carlo simulation of high-energy transport and impact ionization of electrons and holes in Ge, Si, and GaAs," in *SISPAD '96–1996 International Conference on Simulation of Semiconductor Processes and Devices* (IEEE, 1996), pp. 43–44.

¹³C. Jungemann, S. Keith, M. Bartels, and B. Meinerzhagen, "Efficient full-band Monte Carlo simulation of silicon devices," *IEICE Trans. Electron.* **E82C**, 870–879 (1999).

¹⁴J. R. Chelikowsky and M. L. Cohen, "Nonlocal pseudopotential calculations for the electronic structure of eleven diamond and zinc-blende semiconductors," *Phys. Rev. B* **14**, 556–582 (1976).

¹⁵M. L. Cohen and V. Heine, "The fitting of pseudopotentials to experimental data and their subsequent application," *Solid State Phys.* **24**, 37–248 (1970).

¹⁶Y. Zheng, R. Wang, and Y. Li, "The empirical pseudopotential method in the calculation of heterostructure band offsets," *J. Phys.: Condens. Matter* **8**, 7321–7327 (1996).

¹⁷C. May, *Impact Ionization Rate Calculations for Device Simulation* (Diplomarbeit, ETH Zürich, 2005).

¹⁸C. May and F. M. Bufer, "Threshold energy and impact ionization scattering rate calculations for strained silicon," *J. Comput. Electron.* **6**, 23–26 (2007).

¹⁹G. Bulman, V. Robbins, and G. Stillman, "The determination of impact ionization coefficients in (100) gallium arsenide using avalanche noise and photocurrent multiplication measurements," *IEEE Trans. Electron Devices* **32**, 2454–2466 (1985).

²⁰G. Bulman, V. Robbins, K. Brennan, K. Hess, and G. Stillman, "Experimental determination of impact ionization coefficients in (100) GaAs," *IEEE Electron Device Lett.* **4**, 181–185 (1983).

²¹S. Millidge, D. C. Herbert, M. Kane, G. W. Smith, and D. R. Wight, "Non-local aspects of breakdown in pin diodes," *Semicond. Sci. Technol.* **10**, 344–347 (1995).

²²L. W. Cook, G. E. Bulman, and G. E. Stillman, "Electron and hole impact ionization coefficients in InP determined by photomultiplication measurements," *Appl. Phys. Lett.* **40**, 589–591 (1982).

²³K. Taguchi, T. Torikai, Y. Sugimoto, K. Makita, and H. Ishihara, "Temperature dependence of impact ionization coefficients in InP," *J. Appl. Phys.* **59**, 476–481 (1986).

²⁴I. Watanabe, T. Torikai, K. Makita, K. Fukushima, and T. Uji, "Impact ionization rates in (100) Al_{0.48}In_{0.52}As," *IEEE Electron Device Lett.* **11**, 437–438 (1990).

²⁵F. Osaka, T. Mikawa, and T. Kaneda, "Impact ionization coefficients of electrons and holes in (100)-oriented Ga_{1-x}In_xAs_yP_{1-y}," *IEEE J. Quantum Electron.* **21**, 1326–1338 (1985).

²⁶G. Gilat and L. J. Raubenheimer, "Accurate numerical method for calculating frequency- distribution functions in solids," *Phys. Rev.* **144**, 390–395 (1966).

²⁷L. Saravia and J. Duomarco, "The pair scattering and the photoemission effect in GaAs," *J. Phys. Chem. Solids* **34**, 1661–1673 (1973).

²⁸N. Cavassilas, F. Aniel, G. Fishman, and R. Adde, "Full-band matrix solution of the Boltzmann transport equation and electron impact ionization in GaAs," *Solid-State Electron.* **46**, 559–566 (2002).

²⁹D. Harrison, R. Abram, and S. Brand, "Impact ionization rate calculations in wide band gap semiconductors," *J. Appl. Phys.* **85**, 8178–8185 (1999).

³⁰C. Jacoboni and L. Reggiani, "The Monte Carlo method for the solution of charge transport in semiconductors with applications to covalent materials," *Rev. Mod. Phys.* **55**, 645–705 (1983).